Supplementary Information (SI) for Journal of Materials Chemistry C.

Singlet and triplet excitations in chemically functionalized single-walled carbon nanotubes†

Dinesh Thapa,[a,e*], Yulun Han,[b,e] Braden M. Weight,[c] Grace Tiffany,[d,e] Dmitri Kilin,[e] Sergei Tretiak,[c] and Svetlana Kilina[e*]

Supplementary Information

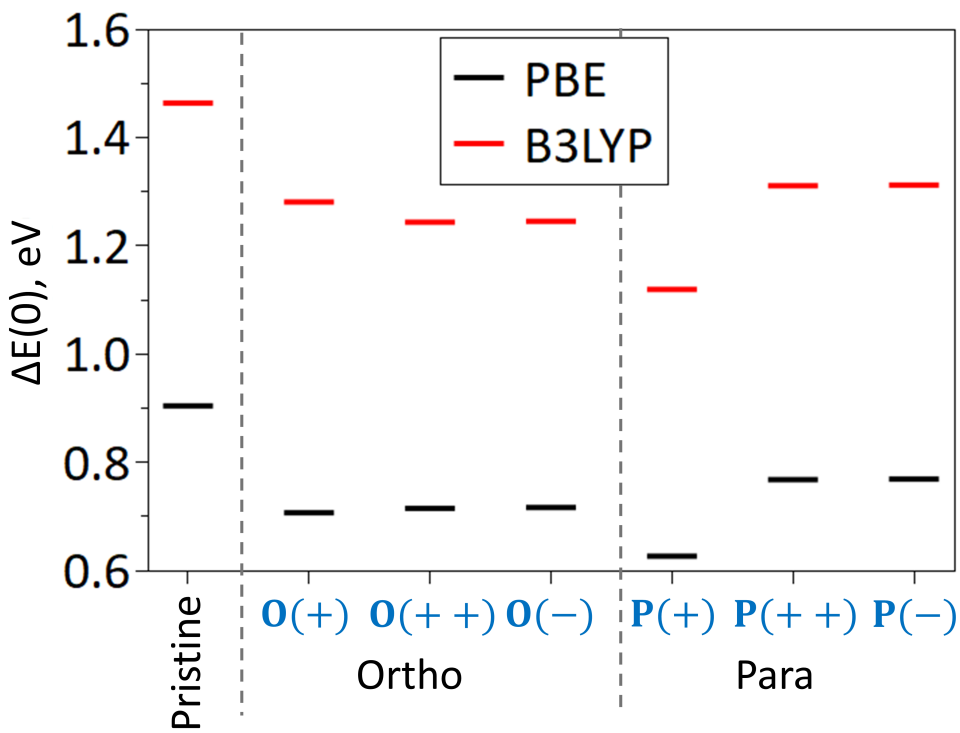

Fig. S1: The HOMO-LUMO gap ($\Delta E(0)$) in the singlet ground state (S_0) for a 10-unit-cell model of the pristine SWCNT and the SWCNT with defects formed by the C_6H_4–NO_2 adduct. Calculations are done at the gamma-kpoint using PBE (black) and B3LYP (red) functionals.

[a] Department of Mathematics and Physics, Thomas More University, Crestview Hills, KY 41017, U.S.A., E-mail: thapad@thomasmore.edu
[b] Department of Natural Sciences, Texas A&M, University - San Antonio, San Antonio, TX 78224, U.S.A.
[c] Theoretical Division, Los Alamos National Laboratory, Los Alamos, NM 87545, U.S.A.
[d] Roy J. Carver Department of Biochemistry, Biophysics and Molecular Biology, Iowa State University, Ames, IA 50011, U.S.A.
[e] Department of Chemistry and Biochemistry, North Dakota State University, Fargo, ND 58102, U.S.A., E-mail: svetlana.kilina@ndsu.edu

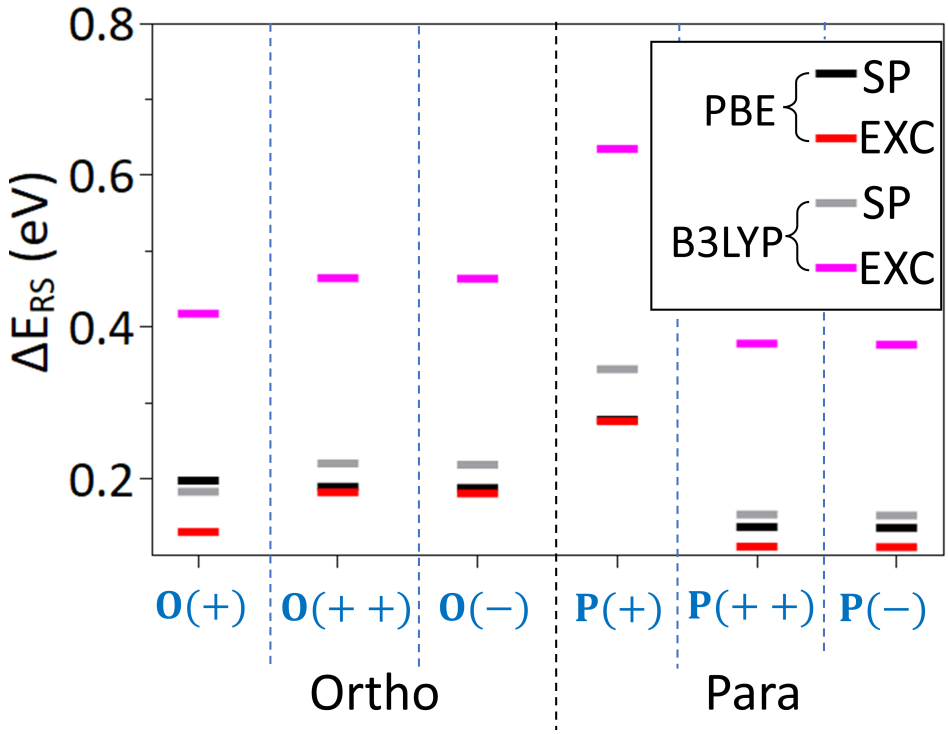

Fig. S2: The optical red shift ($\Delta E_{RS} = E_{11} - E_{11}^{*}$) for six different defect configurations of the (11,0) SWCNT with C_6H_4–NO_2 adduct calculated by the SP and CO-DFT (EXC) methods using PBE and B3LYP functionals. Calculations are performed using the model of 10-unit-cells in length.

Notes and References

1 V. Zólyomi and J. Kürti, *Physical Review B*, 2004, **70**, 085403.

2 K. Kanamitsu and S. Saito, *Journal of the Physical Society of Japan*, 2002, **71**, 483–486.

3 O. Gülseren, T. Yildirim and S. Ciraci, *Physical Review B*, 2002, **65**, 153405.

4 G. Sun, J. Kürti, M. Kertesz and R. H. Baughman, *The Journal of Physical Chemistry B*, 2003, **107**, 6924–6931.

5 D. Dass, *Superlattices and Microstructures*, 2018, **120**, 108–126.

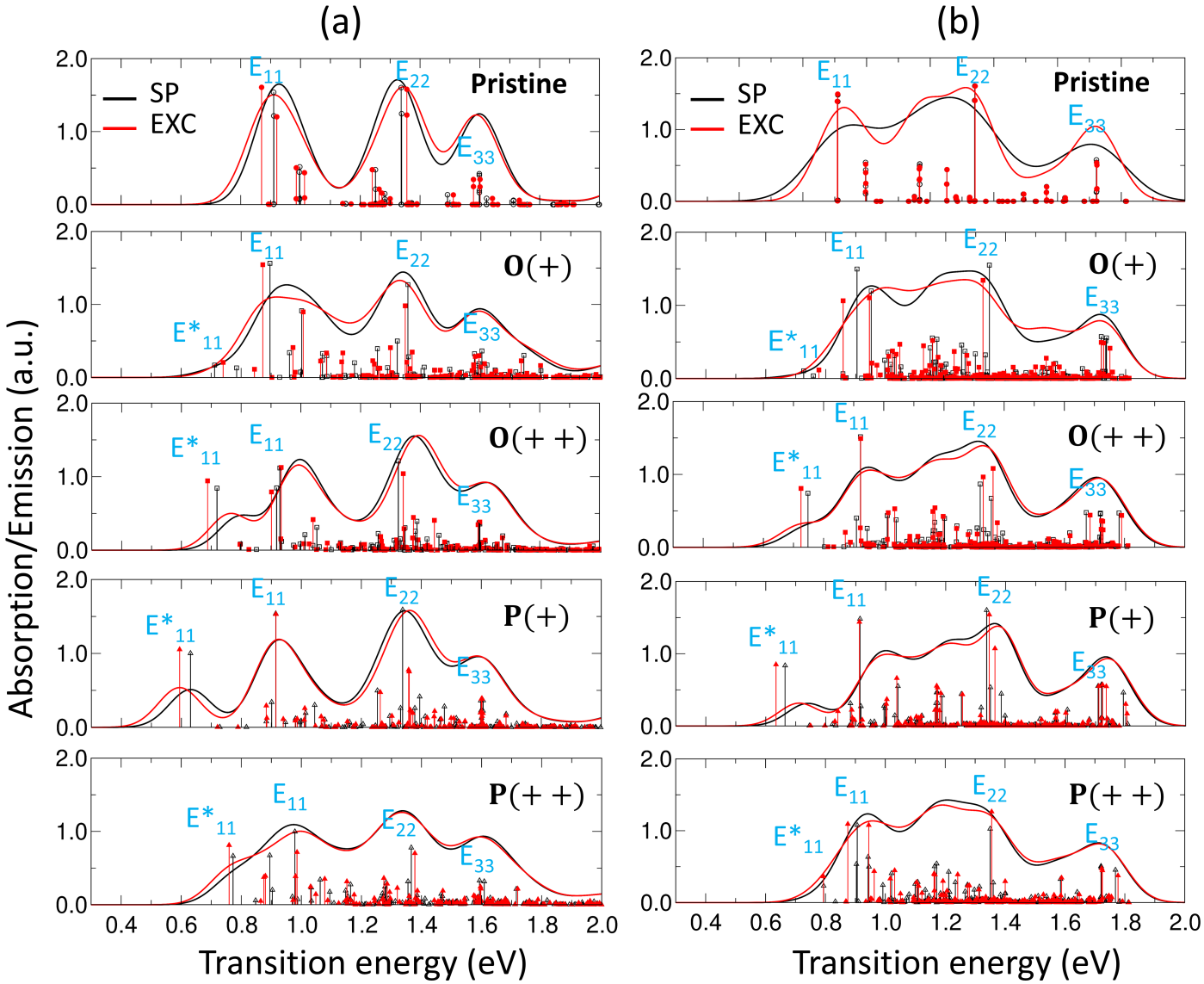

Fig. S3: Optical spectra of the pristine SWCNT and the functionalized SWCNT by C_6H_4–NO_2 adduct at different defect configurations for 10-unit-cell (a) and 18-unit-cell (b) modles calculated by the single-point DFT (SP) and constrained orbit DFT (EXC) using PBE functional. The vertical lines represent the spectral intensities or the oscillator strength of optical transitions contributing to the spectra. The SP method (black lines) approximates the absorption spectra, while the EXC method (red lines) represents the emission spectra.

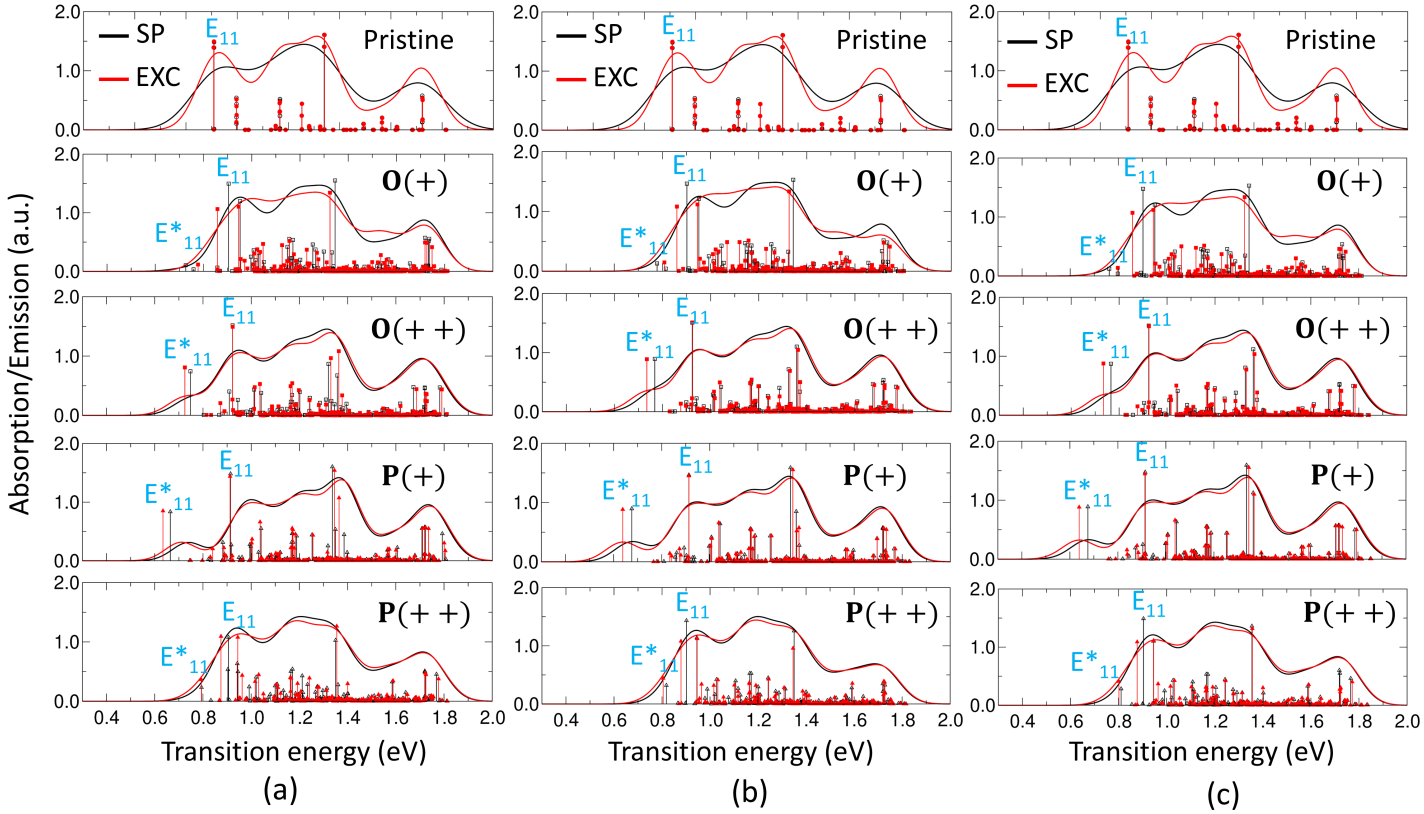

Fig. S4: Optical spectra of pristine SWCNT and SWCNT functionalized by the C_6H_4-R adduct with $R = NO_2$ (a), $R = NH_2$ (b), and $R = H$ (c) at different defect configurations for 18-unit-cell model. Calculations are performed by the single-point DFT (SP) and constrained orbit DFT (EXC) using PBE functional. The vertical lines represent the spectral intensities or the oscillator strength of optical transitions contributing to the spectra. The SP method (black lines) approximates the absorption spectra, while the EXC method (red lines) represents the emission spectra.

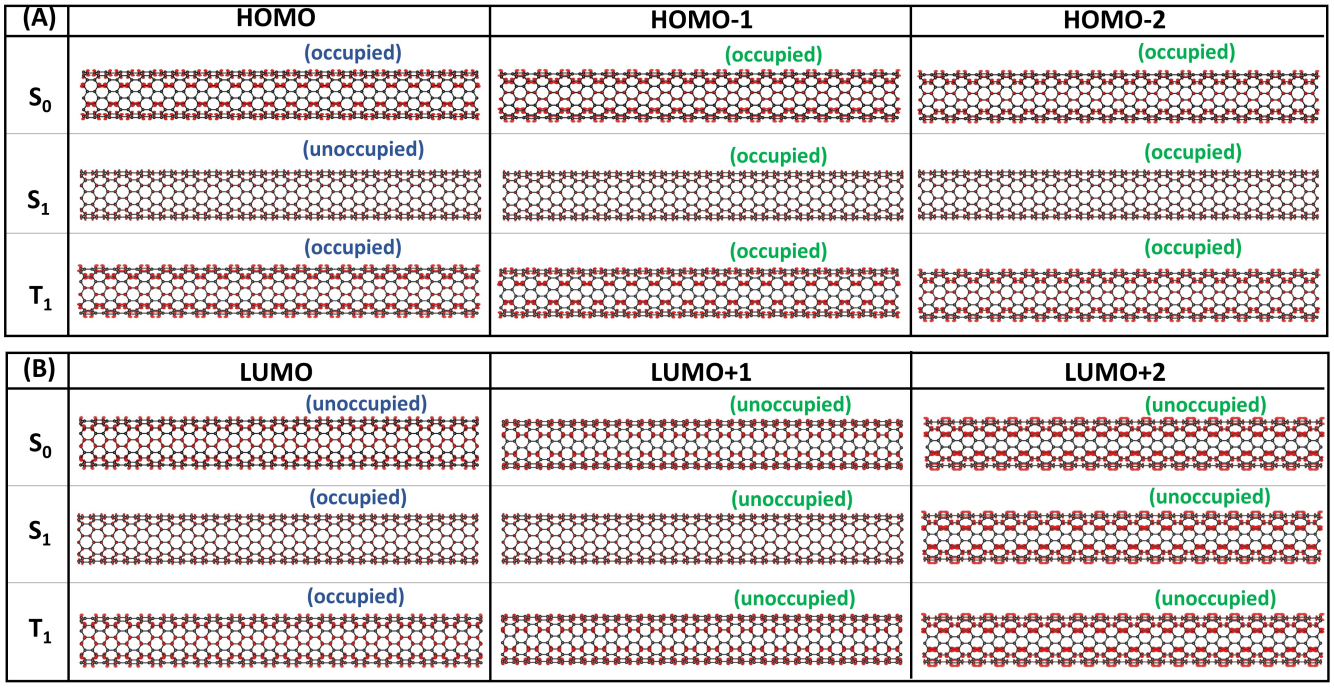

Fig. S5: Partial charge density for a few orbitals contributing to the lowest-energy singlet and triplet optical transitions calculated by the SP (S_0) and CO-DFT (S_1 and T_1) methods for the pristine SWCNT of 18 unit-cell in length using PBE functional.

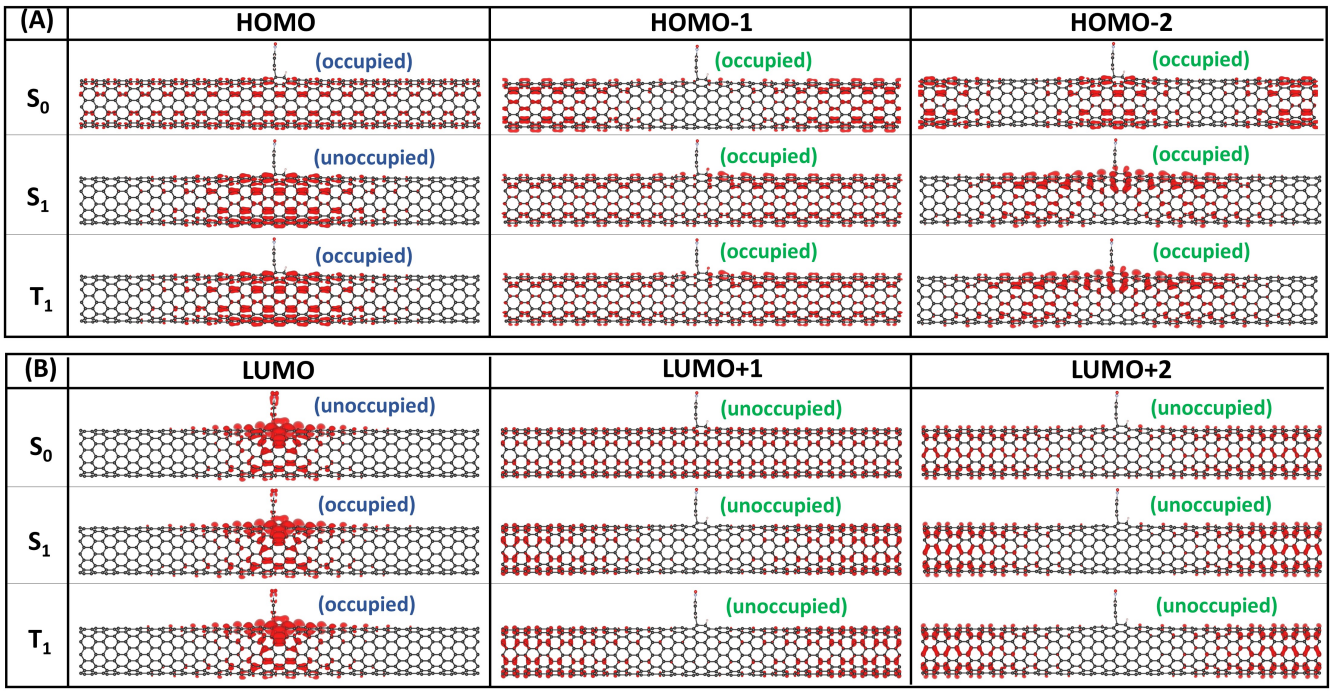

Fig. S6: The same as in Fig. S5 but for the functionalized SWCNT by C_6H_4-NO_2 in the O(+) defect configuration.

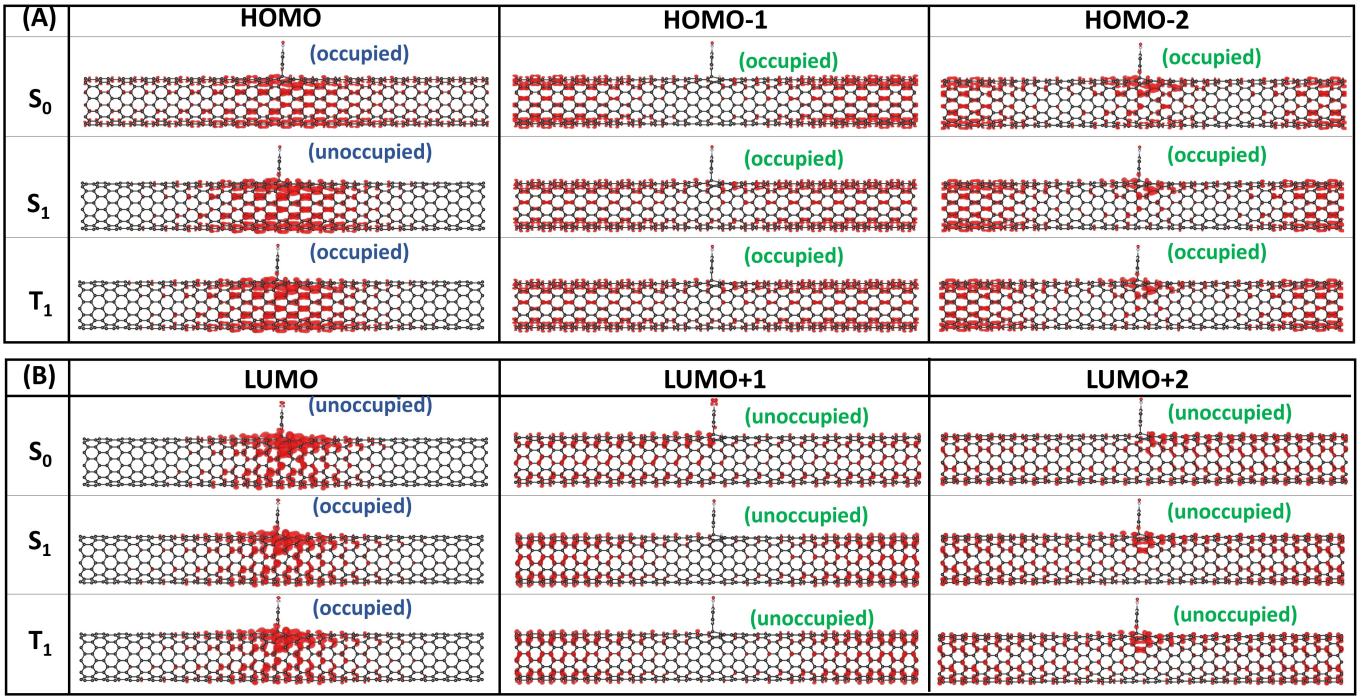

Fig. S7: The same as in Fig. S6, but for the P(++) defect configuration.

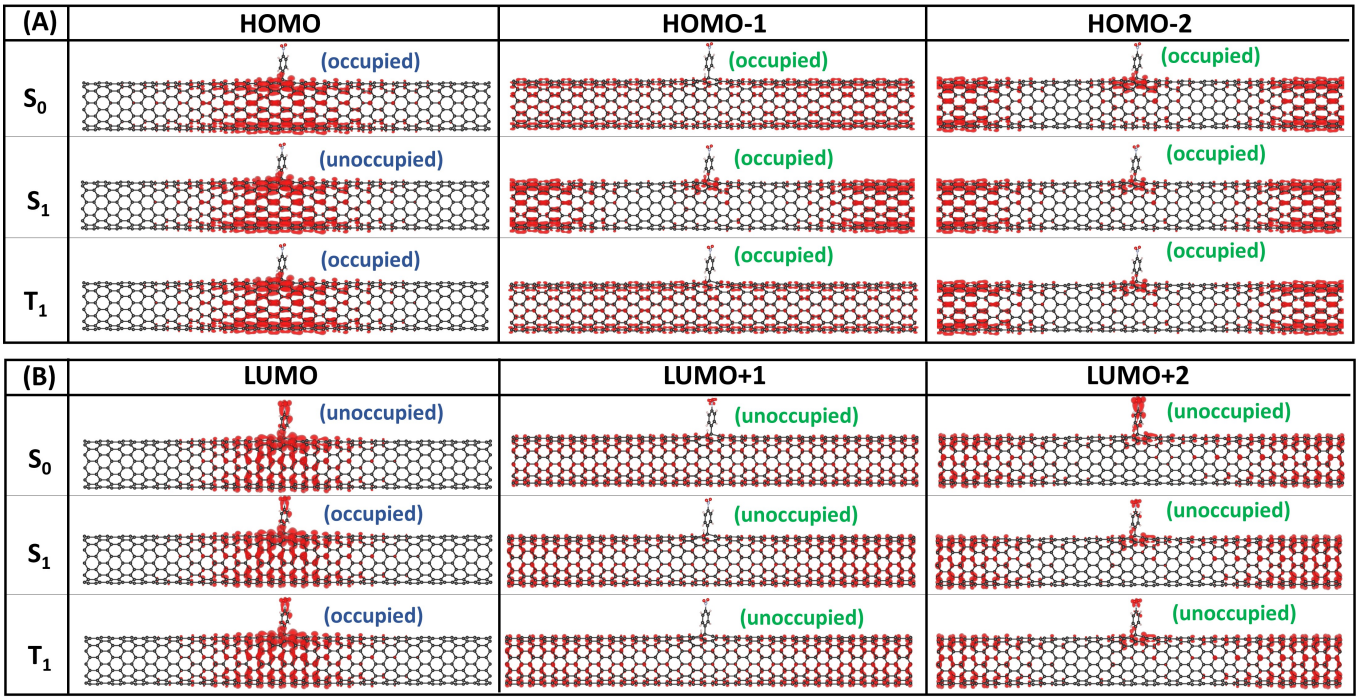

Fig. S8: The same as in Fig. S6 but for the O(++) defect configuration.

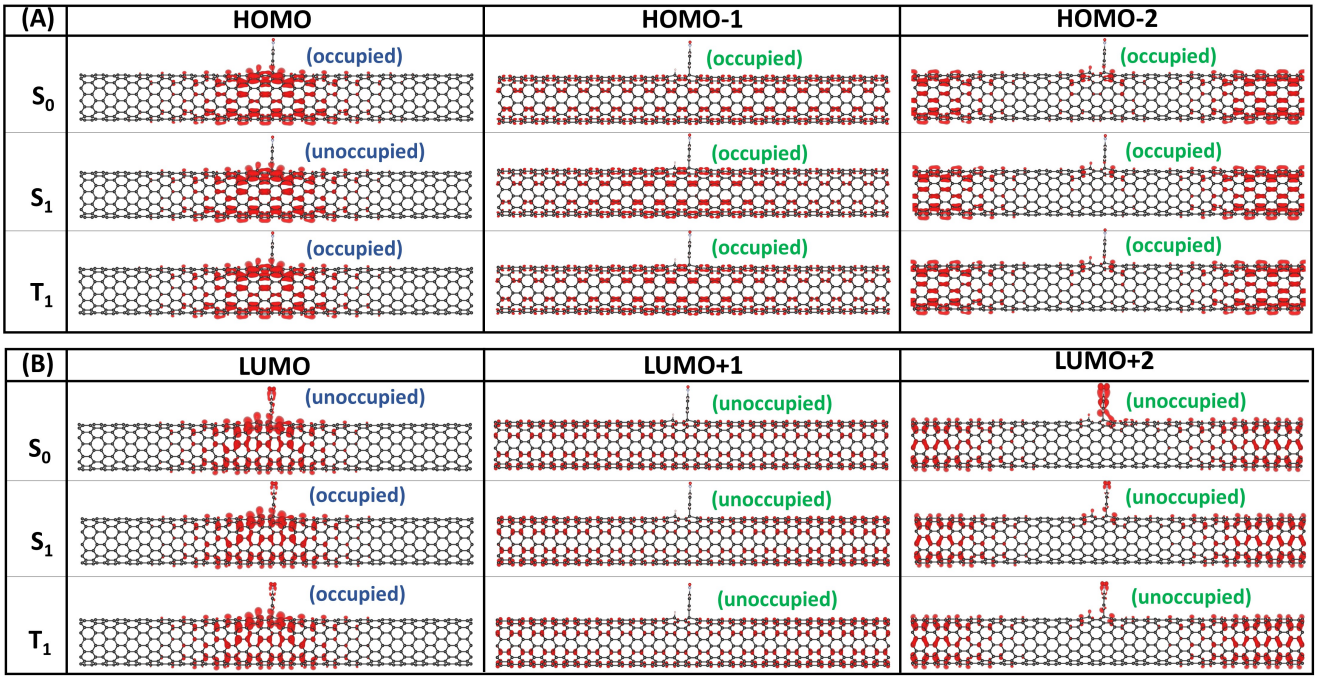

Fig. S9: The same as in Fig. S6, but for the P(+) defect configuration.

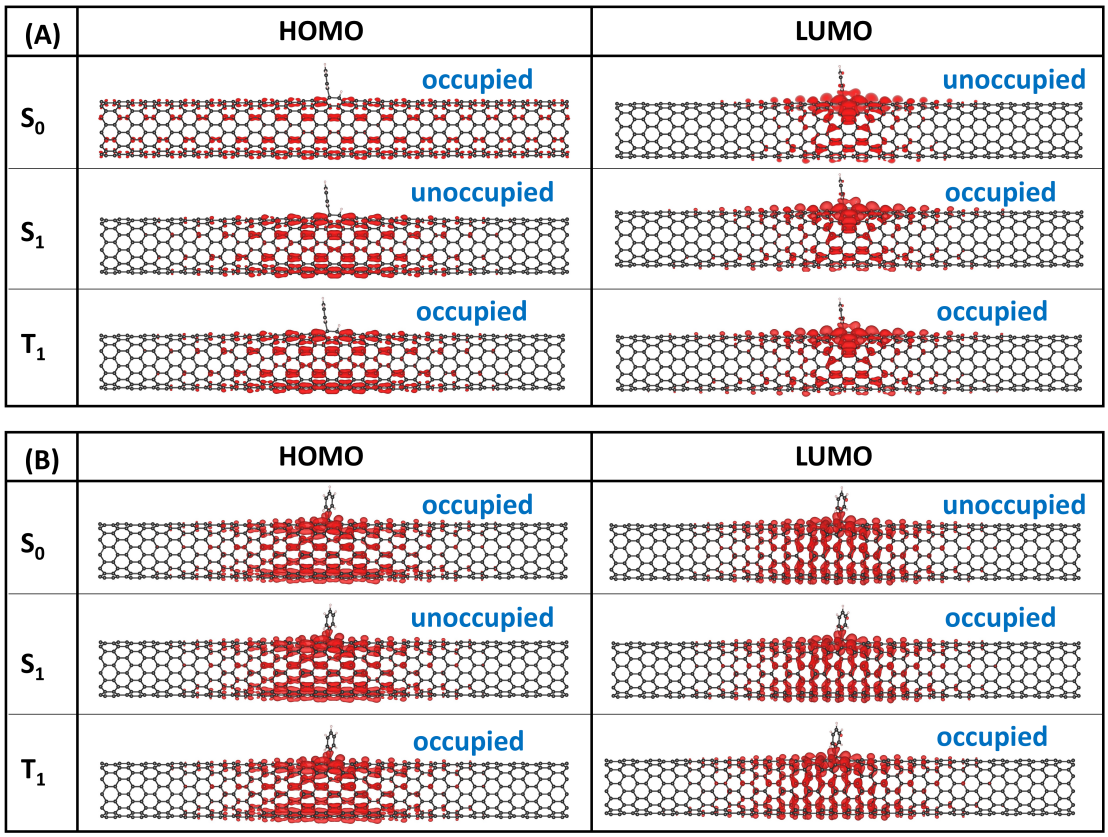

Fig. S10: The same as in Fig. S6 but functionalized by C_6H_4-H adduct in the ortho O(+) **(A)** and O(++) **(B)** defect configurations.

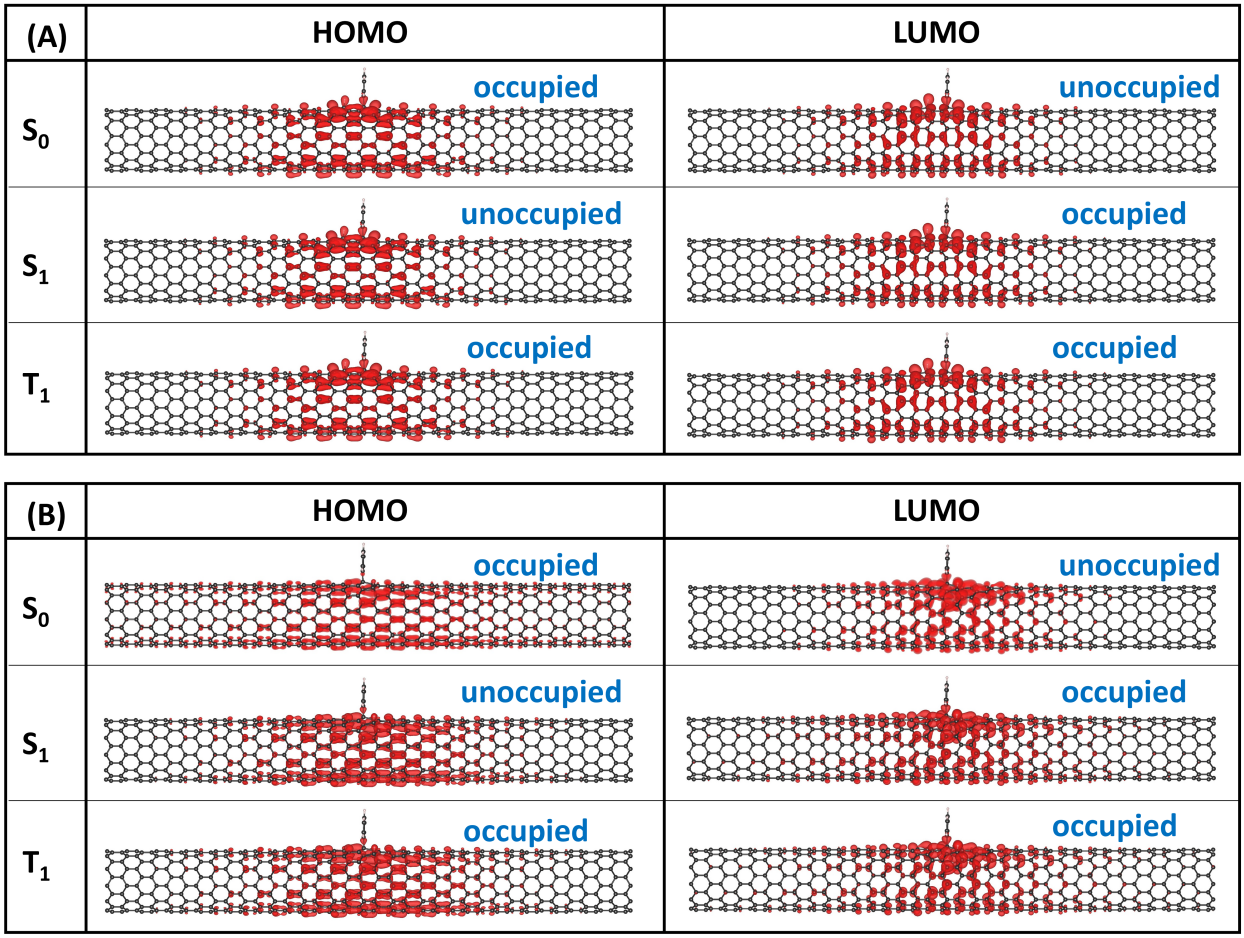

Fig. S11: The same in Fig. S10, but for para P(+) **(A)** and P(++) **(B)** defect configurations.

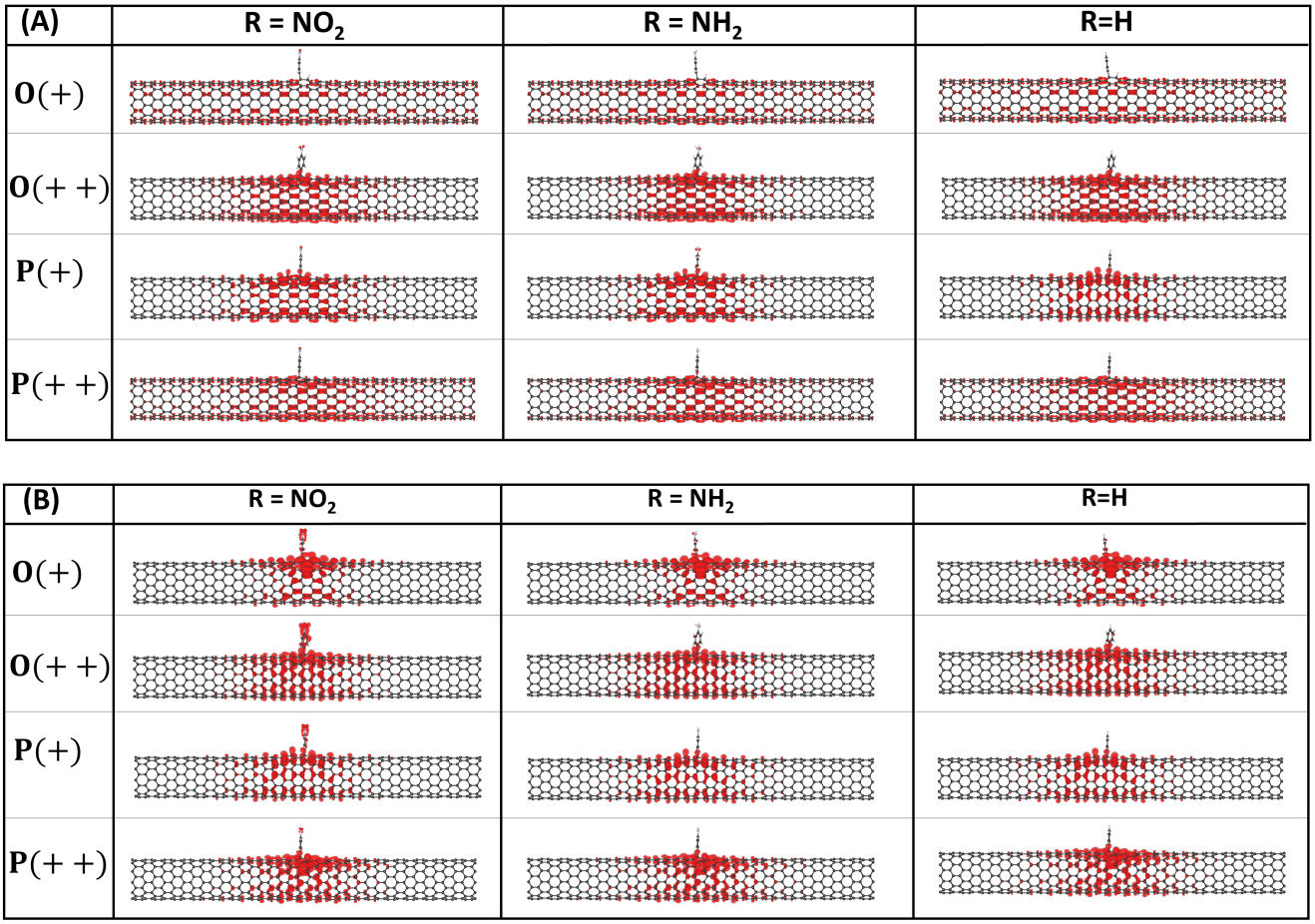

Fig. S12: Partial charge density for HO (occupied) **(A)** and LU (unoccupied) **(B)** orbitals compared between different adduct molecules with $R = NO_2$, NH_2, and H calculated by at the ground S_0 state (SP method) for 18-unit-cell model using PBE functional.

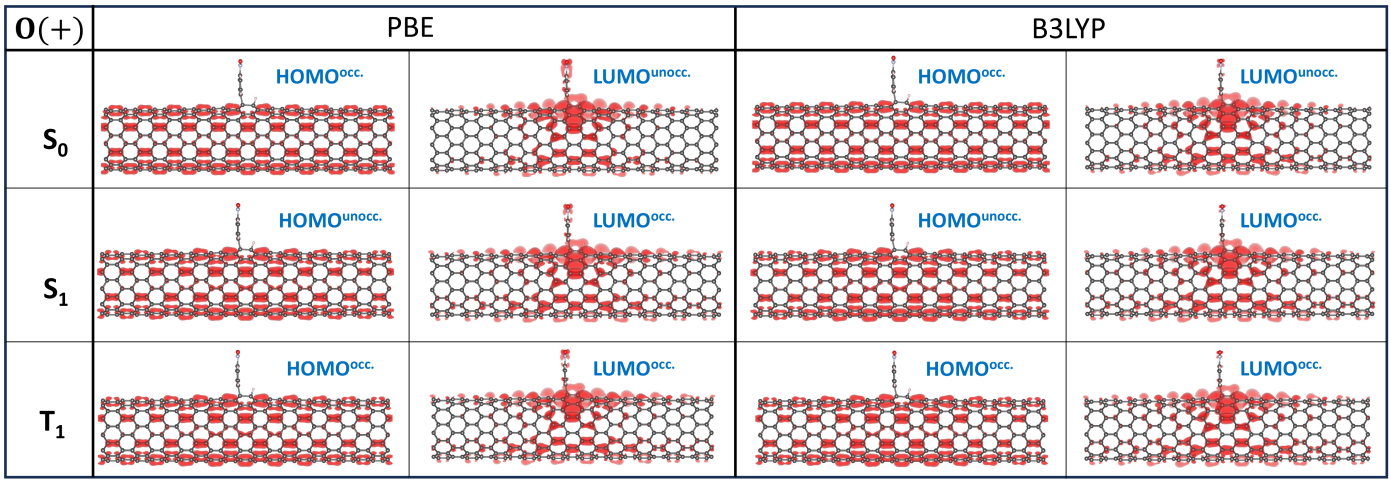

Fig. S13: Partial charge density for a few orbitals contributing to the lowest-energy singlet and triplet optical transitions calculated by the SP (S_0) and CO-DFT (S_1 and T_1) methods for the SWCNT functionalized by C_6H_4–NO_2 of 10-unit cell in length using PBE (left) and B3LYP (right) functionals.

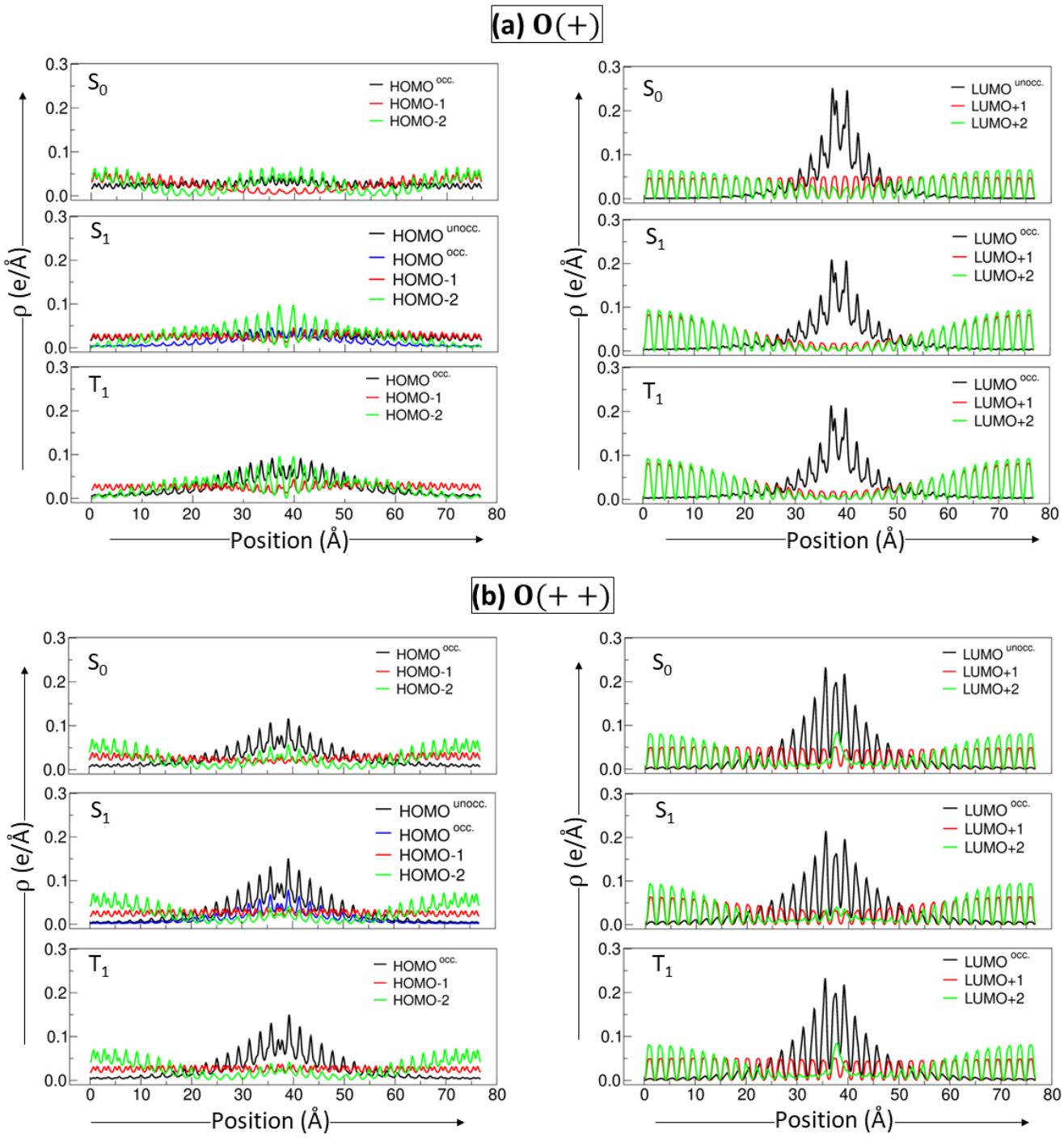

Fig. S14: The linear charge density distributions projected along the nanotube axis for *ortho* defects in the (11,0) SWCNT with C_6H_4-NO_2 adduct. Calculations are performed for 18-unit-cell model using PBE functional. For the singlet exciton (S_1), the superscript "unocc" in HOMO represents a partially populated hole state, while "occ" in LUMO represents a partially populated electron state having an opposite spin than those in HOMO^{unocc}. For the triplet (T_1) exciton, the superscript "occ" in HOMO (hole) and LUMO (electron) defines the partially occupied state, when both have one electron with the same spin. For the singlet ground (S_0) and excited (S_1) states, the superscript "occ" in HOMO represents a fully populated state (with up and down spins), while "unocc" in LUMO represents unoccupied orbital.

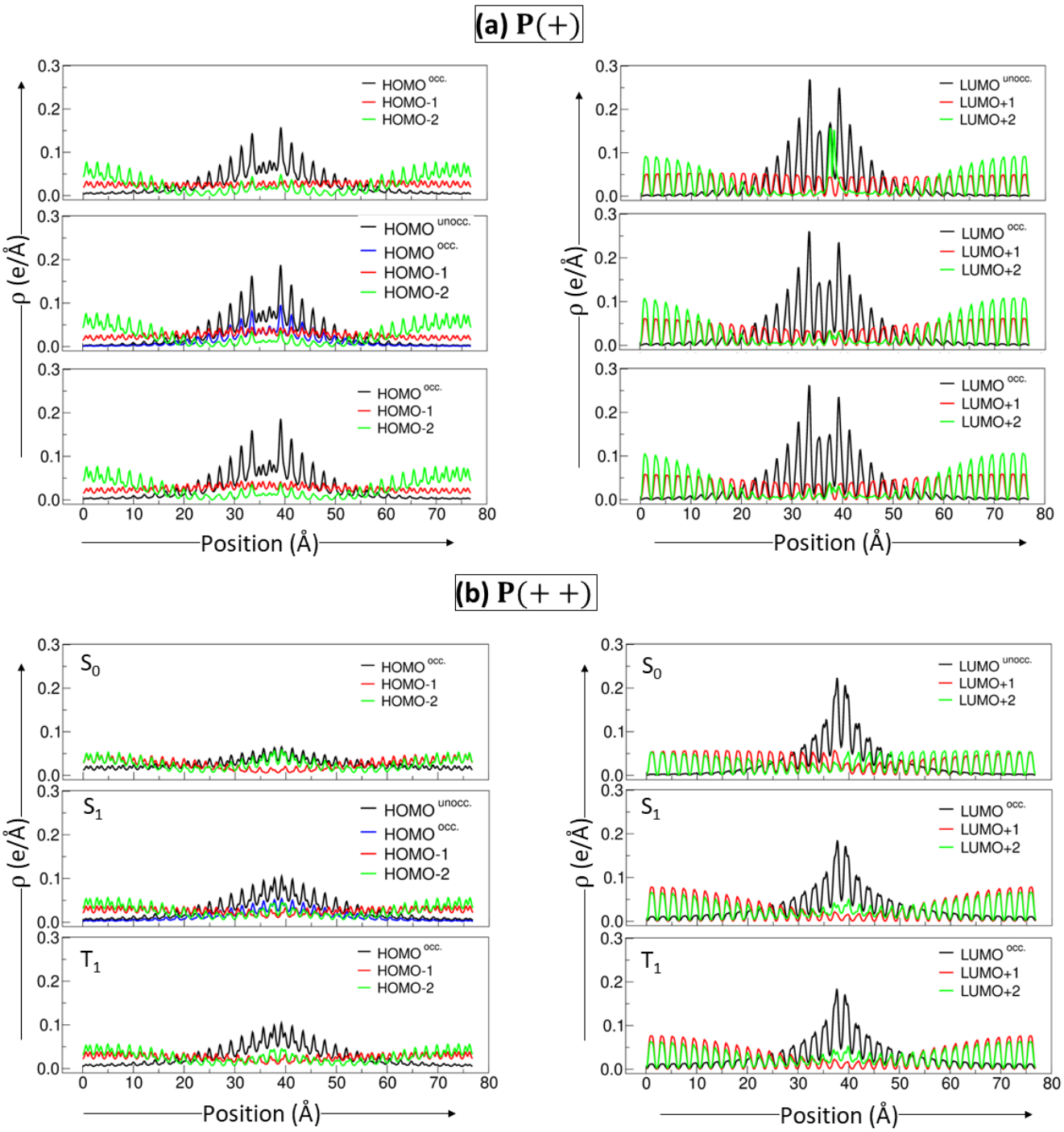

Fig. S15: The same as in Fig. S14 but for *para* defects.

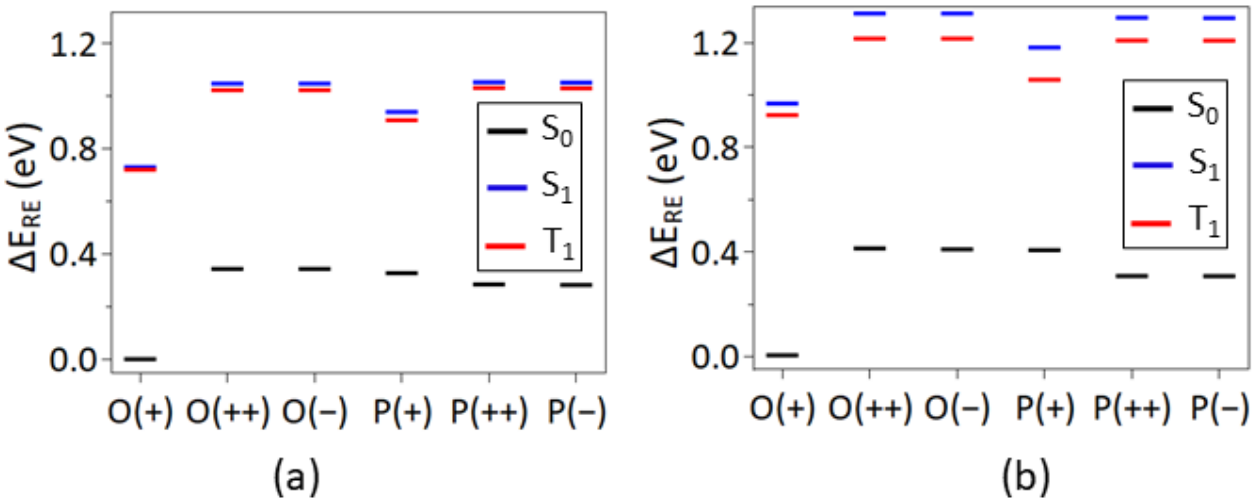

Fig. S16: Relative energy difference of different ortho and para defects, with respect to the most stable configuration O(+), for 10-unit cell $\mathrm{SWCNT}+\mathrm{C_6H_4{-}NO_2}$ calculated by PBE **(a)** and B3LYP **(b)** functionals.

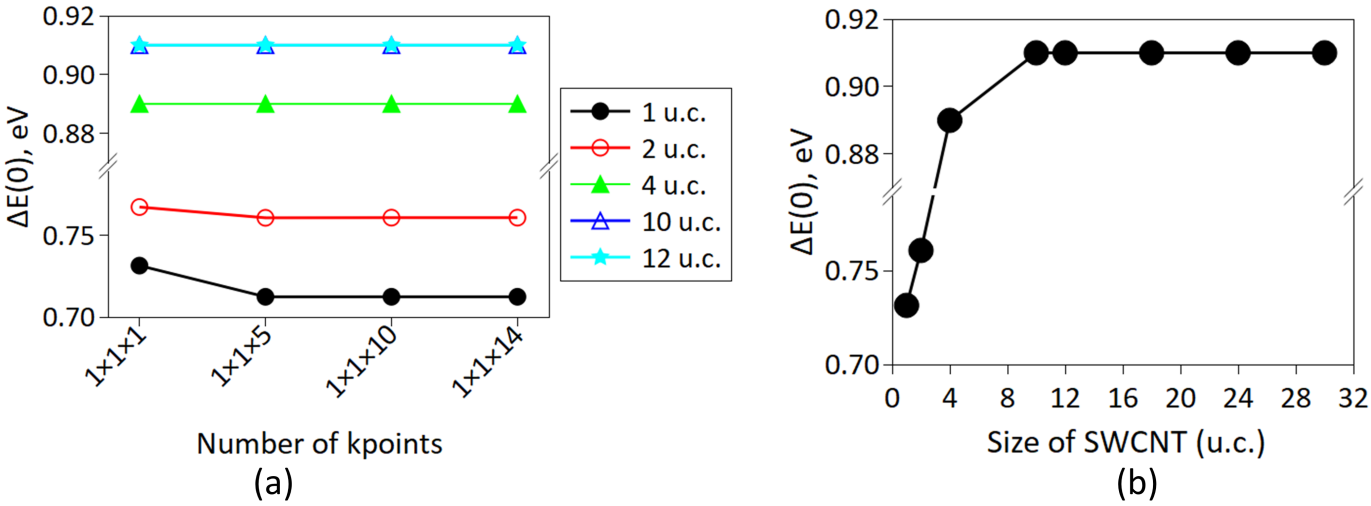

Fig. S17: The band gap $\Delta E(0)$ in the ground state (S_0) for the pristine (11,0) SWCNTs shown as a function of k-points for models of varying lengths (in the number of unit cells (u.c.)) **(a)** and as a function of the model length at Γ-point **(b)**. The calculations are performed using the PBE functional. The $\Delta E(0)$ converges with the increasing number of k-points for the models of shorter length of 1 and 2 u.c, whereas this value is nearly independent of k-points in models larger than 4 u.c. The calculated $\Delta E(0)$ converges to $\sim$ 0.91 eV for the models $\geq$ 10 u.c. This value is in good agreement with reported DFT-based values of 0.93 eV,[1] 1.0 eV[2,3], and 1.13 eV,[4] for the (11,0) SWCNT. Our result is also comparable to the previously reported values of 1.015 eV, and 0.83 eV for the (11,0) SWCNT of 22 u.c. calculated using p_z orbital tight binding (TB) model and Extended Hückel Theory (EHT).[5]

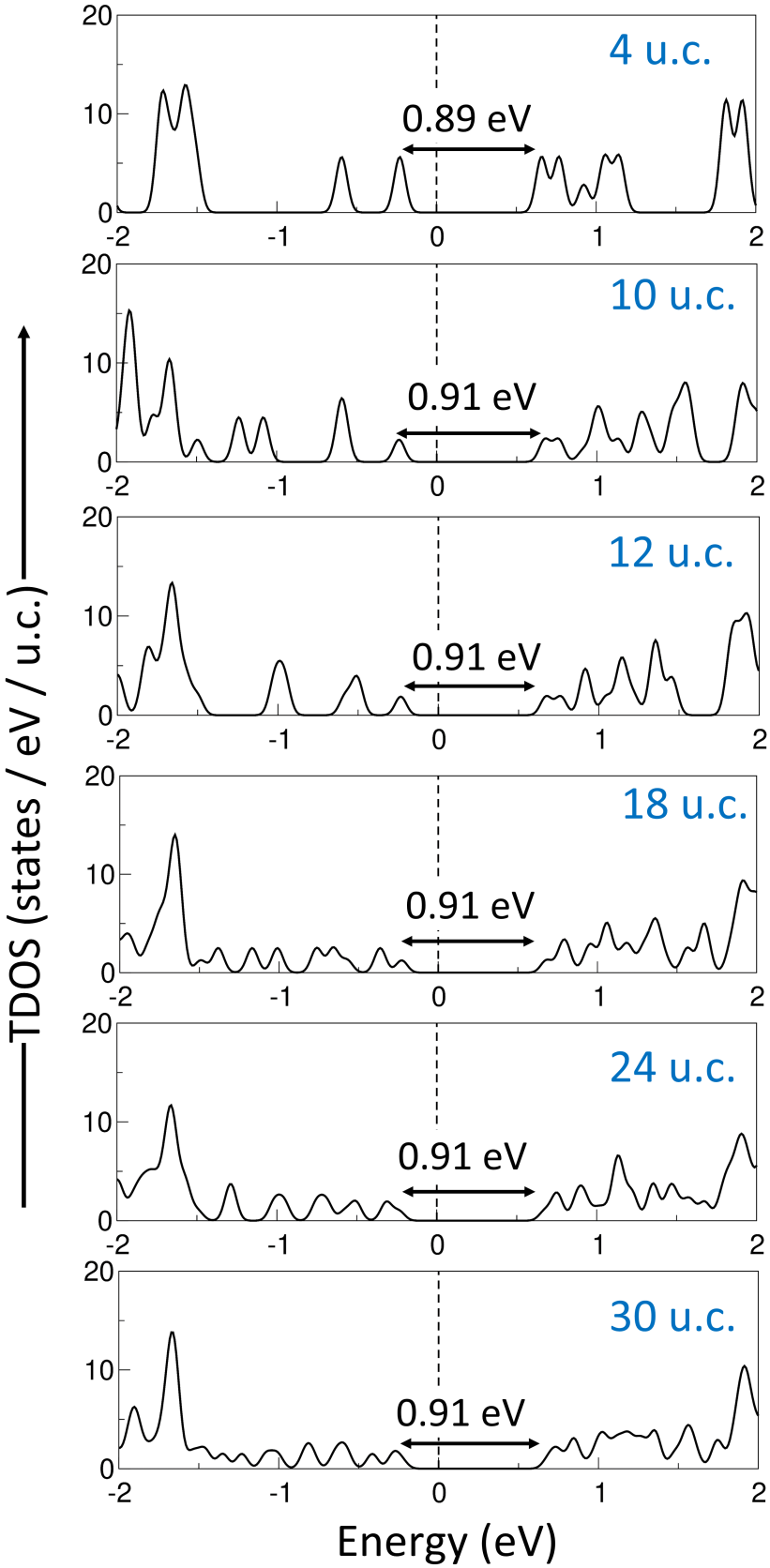

Fig. S18: The total density of states (TDOS) in varying size of pristine SWCNTs calculated using PBE functional at Γ-point of the ground S_0 state. The dashed vertical line in energy scale represents the Fermi energy.

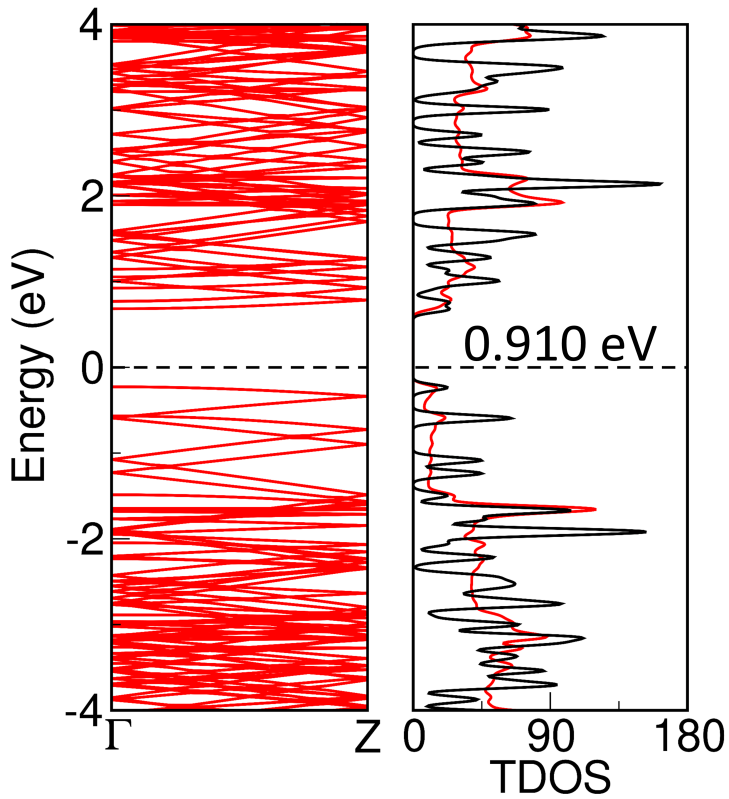

Fig. S19: Electronic band structures along high symmetry kpoints $\Gamma - Z$, and total density of states (TDOS) in eV/states in pristine SWCNT in 10 unit cell size using PBE functional. The TDOS calculated using Gamma k-point only, and averaged over all the k-points are represented by black and red solid lines, respectively. The dashed horizontal black line in energy axis represents the Fermi energy. The number in the inset represents the actual band gap values.

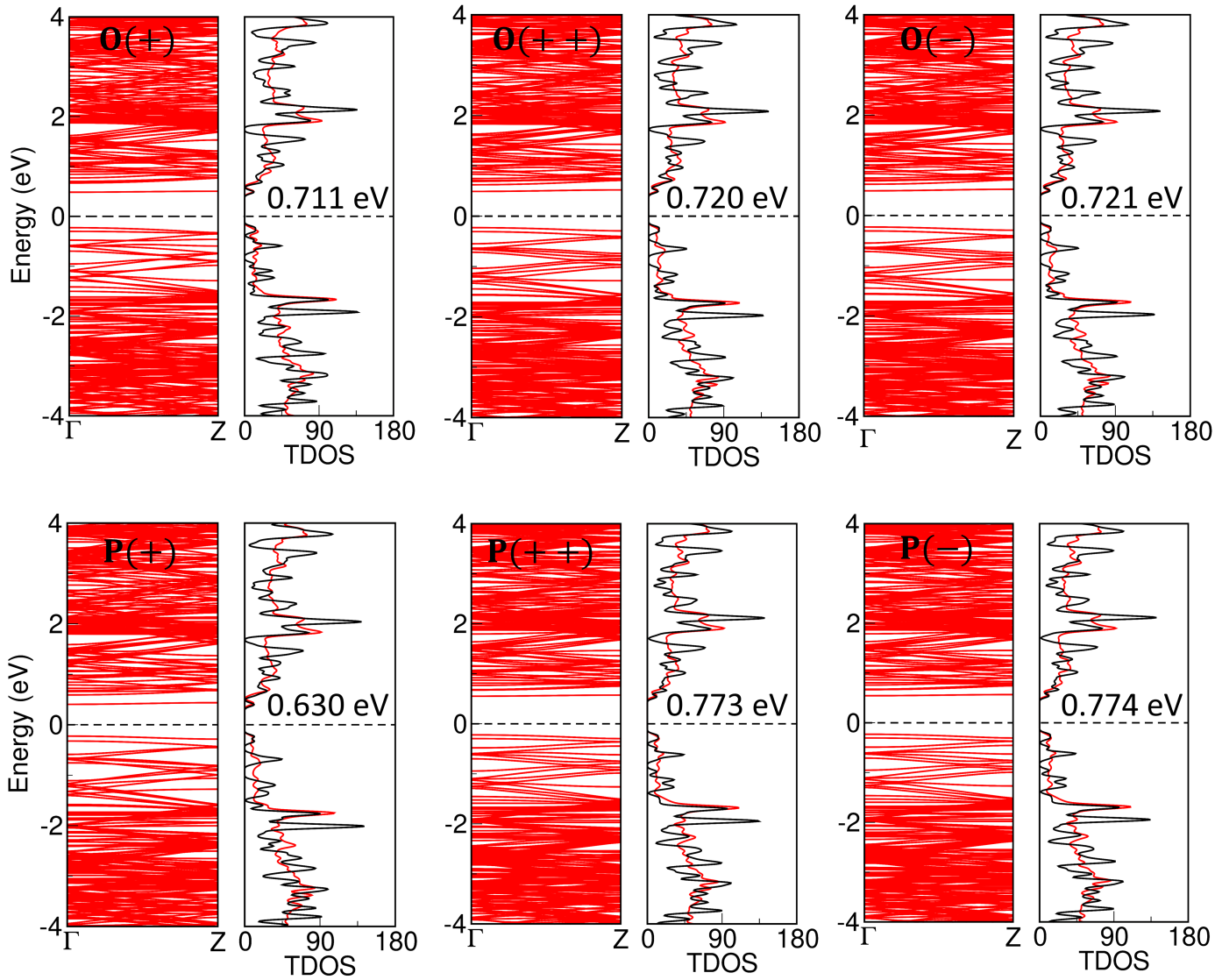

Fig. 20: Electronic band structures along high symmetry kpoints $\Gamma - Z$, and total density of states (TDOS) in eV/states in ortho (O), and para (P) defects in 10 unit cell size SWCNT(11,0)+$C_6H_4 - R$, where $R = NO_2$ in singlet ground S_0 state using PBE functional. The TDOS calculated using Gamma k-point only, and averaged over all the k-points are represented by black and red solid lines, respectively. The dashed horizontal black line in energy axis represents the Fermi energy. The number in the inset represents the actual band gap values.

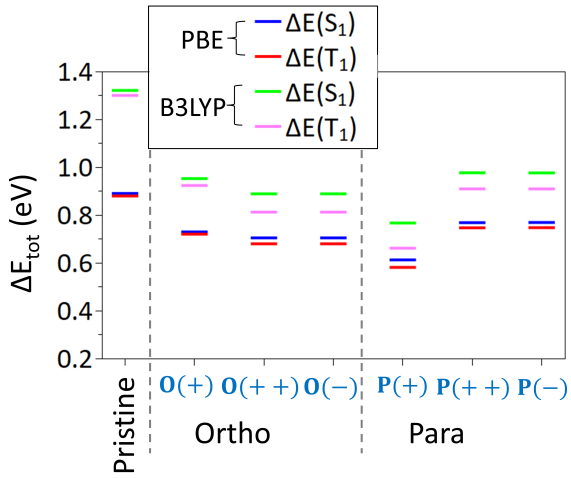

Fig. S21: The non-Aufbau total energy of each system in S_1 and T_1, using the ground state S_0 electronic configuration or geometry as the energy reference represented by $\Delta E(S_1)$ and $\Delta E(T_1)$ using PBE and B3LYP functionals. The calculations were performed for 10 unit cell $\mathrm{SWCNT}+\mathrm{C_6H_4}-\mathrm{R}$, where $\mathrm{R}=\mathrm{NO_2}$.

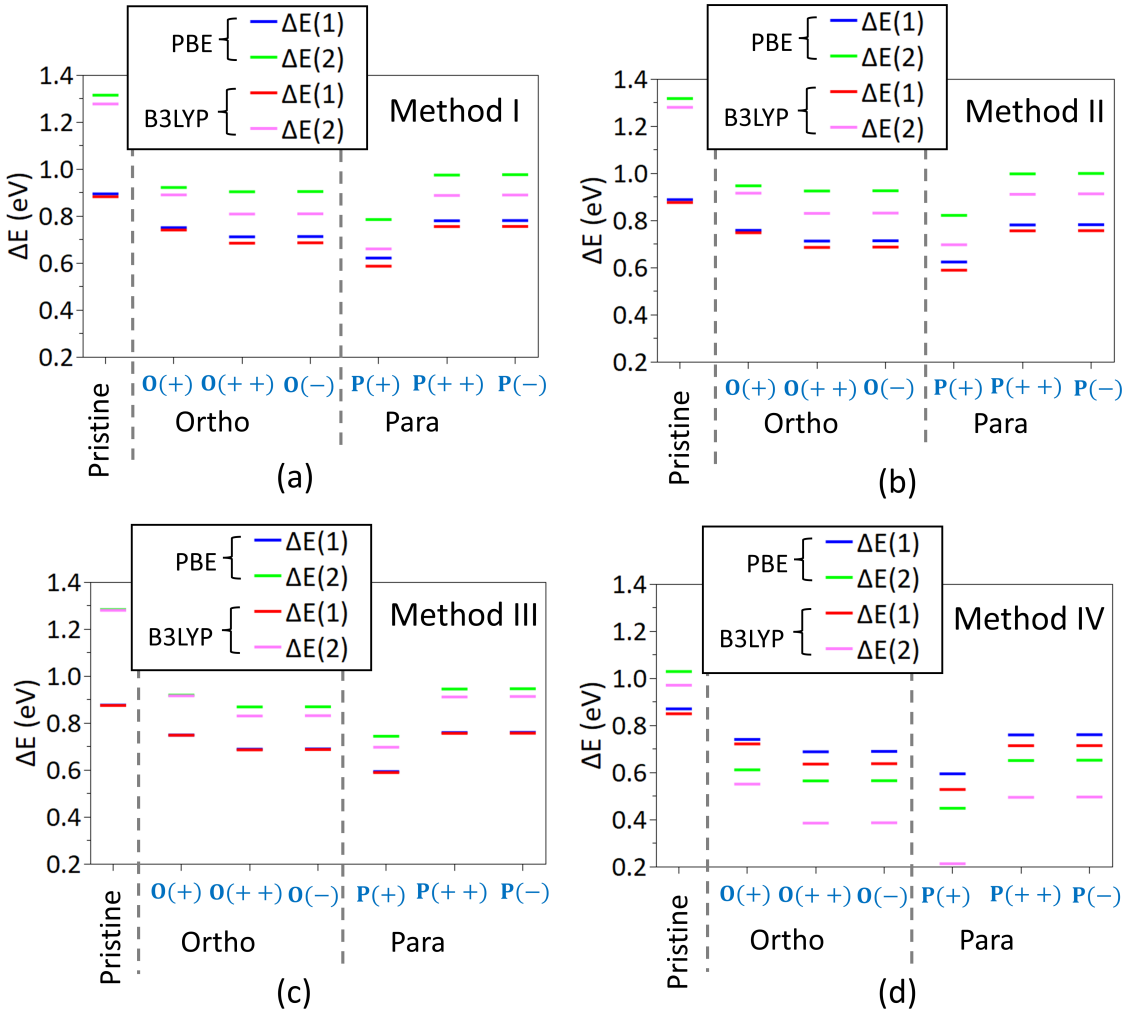

Fig. S22: HO-LU orbital energy gap representing $e-e$ and $e-h$ interactions in S_1 and T_1 with (a) Method-I, (b) Method-II, (c) Method-III, and (d) Method-IV, using PBE and B3LYP functionals. The calculations were performed for 10-unit cell $\mathrm{SWCNT}+\mathrm{C_6H_4}-\mathrm{R}$, where $\mathrm{R}=\mathrm{NO_2}$.

Table 1 Distance (L) in Å between the carbons of the SWCNT with attached adducts (C_6H_4-R and H) creating the sp^3 defects. Calculations are performed by the PBE functional. ΔL represents the change in the L distance between the functionalized and pristine SWCNT.

Size of SWCNT	Structure	Defect	$L(S_0)$	$\Delta L(S_0)$	$L(S_1)$	$\Delta L(S_1)$	$L(T_1)$	$\Delta L(T_1)$
		O(+)	1.5802	0.1592	1.5798	0.1588	1.5797	0.1589
		O(++)	1.6109	0.1899	1.6051	0.1841	1.6040	0.1832
10 u.c.	$R = NO_2$	O(−)	1.6112	0.1902	1.6051	0.1841	1.6044	0.1836
		P(+)	2.8370	−0.0143	2.8358	−0.0155	2.8361	-0.0154
		P(++)	3.0170	0.1657	3.0207	0.1694	3.0208	0.1693
		P(−)	3.0182	0.1669	3.0216	0.1703	3.0218	0.1703
		O(+)	1.5795	0.1585	1.5799	0.1589	1.5806	0.1598
		O(++)	1.6109	0.1899	1.6049	0.1839	1.6040	0.1832
	$R = NO_2$	O(−)	1.6107	0.1897	1.6042	0.1832	1.6033	0.1825
		P(+)	2.8316	−0.0197	2.8310	−0.0203	2.8312	-0.0203
		P(++)	3.0140	0.1627	3.0178	0.1665	3.0181	0.1666
		P(−)	3.0143	0.1629	3.0184	0.1671	3.0187	0.1672
		O(+)	1.5774	0.1564	1.5779	0.1569	1.5779	0.1569
		O(++)	1.6079	0.1869	1.6034	0.1824	1.6028	0.1818
18 u.c.	$R = NH_2$	O(−)	1.6067	0.1857	1.6024	0.1814	1.6017	0.1807
		P(+)	2.8325	−0.0188	2.8308	−0.0205	2.8307	−0.0206
		P(++)	3.0151	0.1638	3.0172	0.1659	3.0170	0.1657
		P(−)	3.0154	0.1641	3.0182	0.1669	3.0185	0.1672
		O(+)	1.5777	0.1567	1.5781	0.1571	1.5781	0.1571
		O(++)	1.6088	0.1878	1.6040	0.1830	1.6033	0.1823
	$R = H$	O(−)	1.6084	0.1874	1.6027	0.1817	1.6027	0.1817
		P(+)	2.8336	−0.0177	2.8325	−0.0188	2.8325	−0.0188
		P(++)	3.0165	0.1652	3.0185	0.1672	3.0186	0.1673
		P(−)	3.0167	0.1654	3.0189	0.1676	3.0188	0.1675

Table 2 The quantitative value of non-Aufbau total energy in eV of each S_1 and T_1 using the ground state S_0 electronic configuration or geometry as the energy reference, represented by $\Delta E(S_1)$, and $\Delta E(T_1)$ respectively. Here, ΔE_{ST} represents the singlet triplet splitting in 18 unit cell SWCNT $+ C_6H_4 - R$, where $R = NO_2$, NH_2, and H using PBE functional.

Structure	Pristine/ Defect	$\Delta E(S_1)$	$\Delta E(T_1)$	ΔE_{ST}
	Pristine	0.9614	0.9439	0.0175
	O(+)	0.7622	0.7402	0.0220
	O(++)	0.7384	0.7121	0.0262
$R = NO_2$	O(−)	0.7383	0.7119	0.0263
	P(+)	0.6463	0.6098	0.0365
	P(++)	0.7965	0.7760	0.0204
	P(−)	0.7966	0.7759	0.0206
	O(+)	0.8009	0.7932	0.0077
	O(++)	0.7511	0.7251	0.0259
$R = NH_2$	O(−)	0.7515	0.7256	0.0259
	P(+)	0.6545	0.6187	0.0358
	P(++)	0.8128	0.7921	0.0207
	P(−)	0.8114	0.7904	0.0210
	O(+)	0.7879	0.7803	0.0076
	O(++)	0.7504	0.7243	0.0261
$R = H$	O(−)	0.7502	0.7239	0.0262
	P(+)	0.6543	0.6193	0.0350
	P(++)	0.8079	0.7873	0.0207
	P(−)	0.8083	0.7874	0.0209

Table 3 The quantitative value of non-Aufbau total energy in eV of each S_1 and T_1 using the ground state S_0 electronic configuration or geometry as the energy reference, represented by $\Delta E(S_1)$, and $\Delta E(T_1)$ respectively. Here, ΔE_{ST} represents the singlet triplet splitting in 10 u.c. $\mathrm{SWCNT} + \mathrm{C_6H_4} - \mathrm{R}$, where $\mathrm{R} = \mathrm{NO_2}$ using PBE and hybrid B3LYP functionals.

Exchange Functional	Pristine/ Defect	$\Delta E(S_1)$	$\Delta E(T_1)$	ΔE_{ST}
	Pristine	0.8900	0.8793	0.0107
	O(+)	0.7292	0.7199	0.0093
	O(++)	0.7041	0.6794	0.0247
PBE	O(−)	0.7041	0.6794	0.0247
	P(+)	0.6122	0.5808	0.0314
	P(++)	0.7679	0.7463	0.0216
	P(−)	0.7686	0.7470	0.0216
	Pristine	1.3208	1.2998	0.0210
	O(+)	0.9520	0.9233	0.0287
	O(++)	0.8884	0.8119	0.0765
B3LYP	O(−)	0.8918	0.8153	0.0765
	P(+)	0.7663	0.6611	0.1052
	P(++)	0.9765	0.9091	0.0674
	P(−)	0.9758	0.9090	0.0668

Table 4 Calculated value of transition energy (E_T) in eV and oscillator strength (f_{pq}) for the lowest HO→LU transition during absorption process in SP (S_0), or LU→HO transition during emission process in EXC (S_1) within 18 unit cell SWCNT + C_6H_4 − R, where R = NO_2, NH_2, and H using PBE functional. Here, the oscillator strength for the degenerate E_{11} and E^*_{11} transitions corresponding to SP and EXC in pristine is calculated taking their average value, while in all other cases the degeneracy is broken. The transition energy E_T in SP and EXC corresponds to the value $E(0)$ and $E(1)$(**Method − IV**), respectively in Table S4.

Structure	Pristine/ Defect	SP (S_0)		EXC (S_1)	
		$E_T(eV)$	f_{pq}	$E_T(eV)$	f_{pq}
	Pristine	0.909	95.998	0.908	72.436
	O(+)	0.726	10.533	0.777	11.743
	O(++)	0.748	74.166	0.725	80.733
$R = NO_2$	P(+)	0.664	83.599	0.634	85.041
	P(++)	0.794	23.216	0.793	36.347
	O(+)	0.778	12.982	0.808	14.704
	O(++)	0.768	89.454	0.735	88.803
$R = NH_2$	P(+)	0.676	89.576	0.638	88.307
	P(++)	0.818	32.049	0.805	44.138
	O(+)	0.762	12.162	0.798	13.693
	O(++)	0.766	87.224	0.734	87.634
$R = H$	P(+)	0.675	88.798	0.639	88.141
	P(++)	0.810	28.244	0.801	41.072

Table 5 Calculated value of transition energy (E_T) in eV and oscillator strength (f_{pq}) for the lowest HO→LU transition during absorption process in SP(S_0), or LU→HO transition during emission process in EXC (S_1) within 10 unit cell SWCNT $+ C_6H_4 - R$, where $R = NO_2$ using PBE and B3LYP functionals. Here, the oscillator strength for the degenerate E_{11} transitions in pristine corresponding to SP is calculated taking their average value, while in all other cases the degeneracy is broken at the transition between frontier orbitals (HO and LU). The transition energy E_T in SP and EXC corresponds to the value $E(0)$ and $E(1)(\textbf{Method} - \textbf{IV})$, respectively in Table S6.

Exchange Functional	Pristine/ Defect	SP (S_0)		EXC (S_1)	
		$E_T(eV)$	f_{pq}	$E_T(eV)$	f_{pq}
PBE	Pristine	0.910	51.65	0.869	160.679
	O(+)	0.711	16.917	0.740	20.562
	O(++)	0.719	84.326	0.688	94.259
	P(+)	0.630	100.168	0.594	105.339
	P(++)	0.773	23.216	0.759	81.218
B3LYP	Pristine	1.463	97.022	1.028	54.183
	O(+)	1.281	12.561	0.611	19.061
	O(++)	1.243	55.280	0.564	100.311
	P(+)	1.119	61.673	0.448	127.537
	P(++)	1.311	45.810	0.650	69.823

Table 6 Table representing HOMO-LUMO energy gap $\Delta E(0)$ in singlet ground (S_0), and HOMO-LUMO energy gap $\Delta E(1)$ and $\Delta E(2)$ in eV showing quantitative value of $e-e$ and $e-h$ interaction in spin polarized singlet ground (S_0), singlet excited (S_1), and triplet (T_1) using 18 u.c. SWCNT $+ C_6H_4 - R$, where $R = NO_2$, NH_2, and H using PBE functional.

Structure	Pristine/ Defect	$\Delta E(0)$	Method I		Method II		Method III		Method IV	
			$\Delta E(1)$	$\Delta E(2)$	$\Delta E(1)$	$\Delta E(2)$	$\Delta E(1)$	$\Delta E(2)$	$\Delta E(1)$	$\Delta E(2)$
	Pristine	0.909	0.908	0.892	0.906	0.889	0.899	0.889	0.908	0.875
	O(+)	0.726	0.805	0.791	0.793	0.779	0.785	0.779	0.777	0.756
	O(++)	0.748	0.755	0.724	0.750	0.719	0.724	0.719	0.725	0.667
$R = NO_2$	O(−)	0.748	0.755	0.723	0.751	0.719	0.725	0.719	0.725	0.667
	P(+)	0.664	0.668	0.625	0.667	0.625	0.632	0.625	0.634	0.559
	P(++)	0.794	0.821	0.794	0.813	0.787	0.792	0.787	0.793	0.747
	P(−)	0.794	0.820	0.794	0.813	0.787	0.792	0.787	0.794	0.747
	O(+)	0.778	0.834	0.826	0.824	0.815	0.816	0.815	0.808	0.792
	O(++)	0.768	0.756	0.728	0.760	0.732	0.736	0.732	0.735	0.678
$R = NH_2$	O(−)	0.768	0.757	0.728	0.761	0.732	0.737	0.732	0.735	0.678
	P(+)	0.676	0.663	0.624	0.672	0.632	0.638	0.632	0.638	0.562
	P(++)	0.818	0.827	0.802	0.824	0.799	0.804	0.799	0.805	0.759
	P(−)	0.818	0.826	0.801	0.823	0.798	0.803	0.798	0.803	0.757
	O(+)	0.763	0.826	0.817	0.814	0.805	0.806	0.805	0.798	0.782
	O(++)	0.766	0.759	0.729	0.759	0.730	0.735	0.730	0.734	0.677
$R = H$	O(−)	0.766	0.759	0.729	0.759	0.730	0.735	0.730	0.734	0.677
	P(+)	0.675	0.668	0.627	0.672	0.632	0.638	0.632	0.639	0.563
	P(++)	0.811	0.825	0.799	0.821	0.796	0.801	0.796	0.801	0.755
	P(−)	0.811	0.826	0.799	0.821	0.795	0.801	0.795	0.801	0.755

Table 7 Calculation of the exchange parameter $\Delta E(1) - \Delta E(2)$ in eV with four different **Methods I-IV** within 18 unit cell SWCNT $+ C_6H_4 - R$, where $R = NO_2$, NH_2, and H using PBE functional.

Structure	Pristine/ Defect	Method I $\Delta E(1) - \Delta E(2)$	Method II $\Delta E(1) - \Delta E(2)$	Method III $\Delta E(1) - \Delta E(2)$	Method IV $\Delta E(1) - \Delta E(2)$
	Pristine	0.015	0.017	0.009	0.033
$R = NO_2$	O(+)	0.014	0.014	0.006	0.021
	O(++)	0.031	0.031	0.005	0.058
	O(−)	0.032	0.032	0.006	0.058
	P(+)	0.043	0.042	0.007	0.075
	P(++)	0.027	0.026	0.005	0.046
	P(−)	0.026	0.026	0.005	0.046
$R = NH_2$	O(+)	0.008	0.009	0.001	0.016
	O(++)	0.028	0.029	0.004	0.057
	O(−)	0.029	0.028	0.005	0.057
	P(+)	0.039	0.039	0.006	0.076
	P(++)	0.025	0.024	0.005	0.046
	P(−)	0.025	0.025	0.005	0.046
$R = H$	O(+)	0.009	0.009	0.001	0.016
	O(++)	0.030	0.029	0.005	0.057
	O(−)	0.030	0.029	0.005	0.057
	P(+)	0.041	0.040	0.006	0.076
	P(++)	0.026	0.025	0.005	0.046
	P(−)	0.027	0.026	0.006	0.046

Table 8 Table representing HOMO-LUMO energy gap $\Delta E(0)$ in singlet ground (S_0), and HOMO-LUMO energy gap $\Delta E(1)$ and $\Delta E(2)$ in eV showing quantitative value of $e-e$ and $e-h$ interaction in spin polarized singlet ground (S_0), singlet excited (S_1), and triplet (T_1) using 10 u.c. SWCNT $+ C_6H_4 - R$, where $R = NO_2$, using PBE and B3LYP functionals.

Exchange Functional	Pristine/ Defect	$\Delta E(0)$	Method I		Method II		Method III		Method IV	
			$\Delta E(1)$	$\Delta E(2)$	$\Delta E(1)$	$\Delta E(2)$	$\Delta E(1)$	$\Delta E(2)$	$\Delta E(1)$	$\Delta E(2)$
	Pristine	0.910	0.894	0.882	0.888	0.876	0.876	0.876	0.869	0.849
	O(+)	0.711	0.750	0.740	0.758	0.748	0.748	0.748	0.740	0.721
	O(++)	0.719	0.711	0.684	0.712	0.685	0.688	0.685	0.688	0.635
PBE	O(−)	0.721	0.712	0.686	0.713	0.687	0.689	0.687	0.689	0.637
	P(+)	0.630	0.621	0.586	0.623	0.589	0.593	0.589	0.594	0.527
	P(++)	0.773	0.779	0.755	0.781	0.756	0.759	0.756	0.759	0.713
	P(−)	0.774	0.781	0.755	0.781	0.756	0.760	0.756	0.760	0.714
	Pristine	1.463	1.314	1.277	1.317	1.279	1.282	1.279	1.028	0.970
	O(+)	1.281	0.921	0.889	0.947	0.915	0.918	0.915	0.611	0.550
	O(++)	1.243	0.903	0.808	0.924	0.829	0.868	0.829	0.564	0.385
B3LYP	O(−)	1.245	0.904	0.809	0.925	0.831	0.869	0.831	0.565	0.386
	P(+)	1.119	0.785	0.659	0.821	0.696	0.743	0.696	0.448	0.212
	P(++)	1.311	0.974	0.887	0.997	0.911	0.944	0.911	0.650	0.494
	P(−)	1.312	0.976	0.889	0.999	0.912	0.945	0.912	0.652	0.496

Table 9 Calculation of the exchange parameter $\Delta E(1) - \Delta E(2)$ in eV with four different **Methods I-IV** within 10 unit cell SWCNT $+ C_6H_4 - R$, where $R = NO_2$ using PBE and B3LYP functionals.

Exchange Functional	Pristine/ Defect	Method I $\Delta E(1) - \Delta E(2)$	Method II $\Delta E(1) - \Delta E(2)$	Method III $\Delta E(1) - \Delta E(2)$	Method IV $\Delta E(1) - \Delta E(2)$
	Pristine	0.012	0.012	0.002	0.021
PBE	O(+)	0.010	0.010	0.001	0.019
	O(++)	0.027	0.027	0.003	0.052
	O(−)	0.026	0.027	0.002	0.052
	P(+)	0.035	0.035	0.004	0.067
	P(++)	0.024	0.025	0.003	0.046
	P(−)	0.026	0.025	0.004	0.046
B3LYP	O(+)	0.037	0.037	0.003	0.058
	O(++)	0.032	0.031	0.003	0.061
	O(−)	0.095	0.095	0.039	0.179
	P(+)	0.126	0.125	0.047	0.236
	P(++)	0.087	0.087	0.033	0.156
	P(−)	0.087	0.086	0.033	0.156